ELSEVIER

Journal of Power Sources 105 (2002) 161–168

JOURNAL OF POWER SOURCES

www.elsevier.com/locate/jpowsour

Investigation of new types of lithium-ion battery materials

Bruno Scrosati*, Stefania Panero, Priscilla Reale, Daniela Satolli, Yuichi Aihara[1]

Dipartimento di Chimica, Università "La Sapienza", 00185 Rome, Italy

Abstract

This paper reports part of the activities in progress in our laboratory in the investigation of electrode and electrolyte materials which may be of interest for the development of lithium-ion batteries with improved characteristics and performances. This investigation has been directed to both anode and cathode materials, with particular attention to convertible oxides and defect spinel-framework Li-insertion compounds in the anode area and layered mixed lithium–nickel–cobalt oxide and high voltage, metal type oxides in the cathode area. As for the electrolyte materials, we have concentrated the efforts on composite polymer electrolytes and gel-type membranes. In this work we report the physical, chemical and electrochemical properties of the defect spinel-framework Li-insertion anodes and of the high voltage, mixed metal type oxide cathodes, by describing their electrochemical properties in cells using either "standard" liquid electrolytes and "advanced" gel-type, polymer electrolytes.

The results illustrated here demonstrate that the spinel-framework anodes of the $Li[Li_{1/3}Ti_{5/3}]O_4$ type can be combined with high voltage cathodes of the $Li_2M_xMn_{(4-x)}O_8$ family for the fabrication of new types of lithium-ion battery systems cycling around 3.5 V. The development of this interesting concept is however still limited by the availability of highly stable electrolytes. © 2002 Published by Elsevier Science B.V.

Keywords: Lithium-ion; Anodes; Cathodes; Electrolytes; Batteries

1. Introduction

Lithium-ion batteries, namely the high energy power sources based on a carbonaceous (i.e. graphite or coke) anode, a lithium metal oxide (e.g. $LiCoO_2$) cathode and a liquid (e.g. a solution of $LiPF_6$ in a ethylene carbonate–dimethylcarbonate, EC–DMC mixture) electrolyte [1,2] are presently the power sources of choice in the consumer electronics market. Accordingly, lithium-ion batteries are today produced at a rate of several million of units per month, mostly by Japanese manufacturers, and they are acquiring a prominent role as ideal systems for powering sophisticated portable devices, such as high technology cellular phones and lap-top computers [3,4].

However, although a commercial reality, the lithium-ion battery is still the object of intense R&D aimed to further improve its performance. The areas of interest extend on all the three main battery components, i.e. anode, cathode and electrolyte. In line with this tendency, in the latest years we have carried out a systematic investigation on those materials which appear particularly promising for the development of lithium-ion batteries with improved characteristics and performances. In the electrode area the investigation has included both anode and cathode materials. In particular, we have synthesized non-carbonaceous alloys formed by convertible oxides, e.g. SnO_2 [5,6] and defect spinel-framework Li-insertion compounds, e.g. $Li[Li_{1/3}Ti_{5/3}]O_4$ [7,8]. The studies on cathode materials have been focused on the characterization of layered mixed lithium–nickel–cobalt oxide, $LiNi_yCo_{(1-y)}O_2$ [9,10] and of high voltage, mixed metal type oxides, e.g. $LiNi_yCo_{(1-y)}VO_4$ [11] and $Li_2M_xMn_{(4-x)}O_8$ [12]. In the electrolyte area we have concentrated the efforts on composite membranes obtained by dispersing selected ceramic powders both in poly(ethylene oxide) PEO-LiX [13,14] polymer electrolytes [13,14] and in poly(acrylonitrile) PAN-based gels [15,16]. In this paper, we describe the progresses achieved on the defect spinel-framework Li-insertion anodes and on the high voltage, mixed metal type oxide cathodes, by reporting their electrochemical properties in cells using either "standard" liquid electrolytes or "advanced" gel-type, polymer electrolytes.

2. Experimental

The spinel-type $Li[Li_{1/3}Ti_{5/3}]O_4$ anode material and the spinel solid solution $Li_2Co_{0.4}Fe_{0.4}Mn_{3.2}O_8$ cathode material were both synthesized using a wet dissolution procedure

* Corresponding author. Tel.: +39-06-491769; fax: +39-06-4462866.
E-mail address: scrosati@uniroma1.it (B. Scrosati).
[1] On leave from Yuasa Corporation, Osaka, Japan.

0378-7753/02/$ – see front matter © 2002 Published by Elsevier Science B.V.
PII: S0378-7753(01)00935-1

optimized in our laboratory. Basically, $Li[Li_{1/3}Ti_{5/3}]O_4$ was prepared by dispersing stoichiometric amount of TiO_2 (Anatase, Aldrich 99.9%) and $LiOH{\cdot}H_2O$ (Aldrich) in *n*-hexane. After removing the solvent, the resulting powder has been ground and calcined at 800 °C for 24 h under oxygen flux.

The synthesis of $Li_2Co_{0.4}Fe_{0.4}Mn_{3.2}O_8$ involved the mixing of water–acetic acid solutions of the precursors, i.e. $LiOH{\cdot}H_2O$ (Fluka), $Mn(CH_3COO)_2{\cdot}4H_2O$ (Aldrich), $Co(NO_3)_2{\cdot}6H_2O$ (Fluka) and $Fe(NO_3)_3{\cdot}9H_2O$ (Aldrich), followed by the evaporation to dryness and the annealing of the resulting powders. The solutions were stirred and evaporated to dryness at 120 °C. The resulting powders were ground and pre-calcined in air at 200 °C for 2 h and at 300 °C for 10 h. The solids were crushed and annealed under oxygen flux at 800 °C for 24 h with slow-cooling and intermittent regrinding.

The stoichiometry and the structure of the final anode and cathode compounds were determined by plasma atomic emission (IPC) and by X-ray powder diffraction (XRPD) analyses, respectively. Figs. 1 and 2 show the related X-ray spectra: the patterns reveal the high degree of crystallinity of the samples and confirm the purity and the high crystallinity of the two-electrode compounds.

In view of their electrochemical characterization, these compounds were shaped in the form of film electrodes by blending them in mixture with a polyvynilidene fluoride (PVdF) binder (about 5 wt.%) and a carbon (Super P) electronic conductor (about 5 wt.%). The slurry was then cast onto an Al foil (in the cathode case) or onto a Cu foil (in the anode case) to form the desired electrode films.

Two types of liquid electrolytes were used for the electrochemical tests, i.e. a solution of 1 M $LiClO_4$ in 1:1 ethylene carbonate–propylene carbonate, EC–PC (Merck Battery Grade) preferentially used for the $Li[Li_{1/3}Ti_{5/3}]O_4$ electrochemical cells, and a solution of 1 M $LiPF_6$ in propylene carbonate, PC (Merck Battery Grade) mostly used for the high voltage, $Li_2Co_{0.4}Fe_{0.4}Mn_{3.2}O_8$ electrode study. The basic electrochemical investigation was carried out in three-electrode cells using lithium as both the counter and the reference electrode. The charge–discharge tests were run with two-electrode coin cells formed by contacting in sequence the given electrode film, a felt separator disk soaked with the given electrolyte solution and a lithium disk counter electrode.

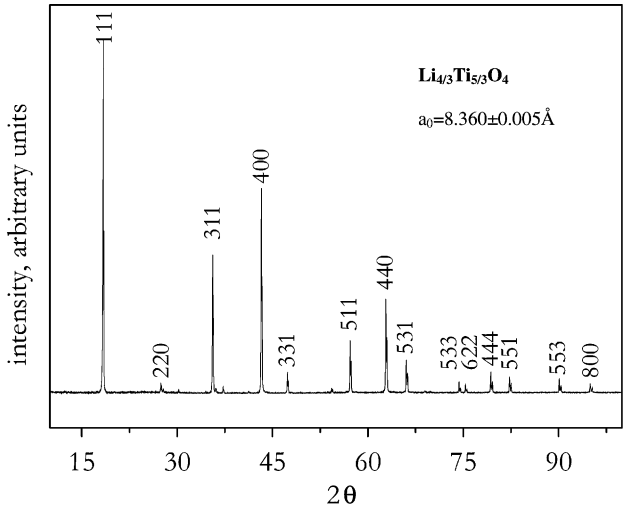

Fig. 1. X-ray powder diffraction patterns of the $Li[Li_{1/3}Ti_{5/3}]O_4$ compound.

The electrochemical tests were extended to polymer electrolyte cells where the given electrode film was separated from the lithium counter electrode by a polymer membrane. The latter was formed by gelling the above mentioned liquid solutions in a poly(acrilonitrile) PAN, polymer matrix. The preparation procedure, specifically developed in our laboratory, involved a sequence of steps (all carried out inside an environmentally controlled dry-box) which included: (i) the dissolution at room temperature of the selected lithium salt ($LiClO_4$) in the given organic solvent mixture (EC–PC); (ii) the addition of the PAN polymer component and its dispersion in the solution by stirring for several hours at room temperature; (iii) the very short-time (about 30 s) transfer of the slurry formed on an aluminum plate preheated at 90 °C for promoting a fast and complete dissolution; (iv) the cooling of the solution to room temperature to favor cross-linking in the membrane and gel formation. Occasionally, nanometric fillers were added during step (ii) in order to obtain composite membranes [17].

This optimized synthesis procedure gives homogeneous and mechanically stable (free standing), 100 μm average thickness membranes, which hereafter will be simply indicated by listing the components in sequence, e.g. $LiClO_4$–EC–PC–PAN.

All the manipulations and the cell assemblages were carried out in a Braun type Labmaster 130 dry-box. The electrochemical tests were performed using an AMEL 2051 potentiostat coupled with an AMEL 568 function generator for the electrode cycling voltammetry, and a MACCOR automatic cycler for the battery cycling. The impedance spectroscopy was carried out with a Solartron, Mod. 1260 frequency response analyzer.

3. Results and discussion

The $Li[Li_{1/3}Ti_{5/3}]O_4$ compounds are of current interest as new types of negative electrodes in advanced, lithium-ion battery structures [18,19]. These compounds adopt a defect spinel-framework structure which is capable of accepting and releasing lithium without noticeable changes in the lattice dimension. Indeed, by an in-situ energy dispersive X-ray diffraction analysis optimized in our laboratory [20], we have been able to show that the lithium intercalation–de-intercalation process in $Li[Li_{1/3}Ti_{5/3}]O_4$ is accompanied by an extremely small variation of the host lattice parameter, i.e. confined between 1% [8] over the entire cycle.

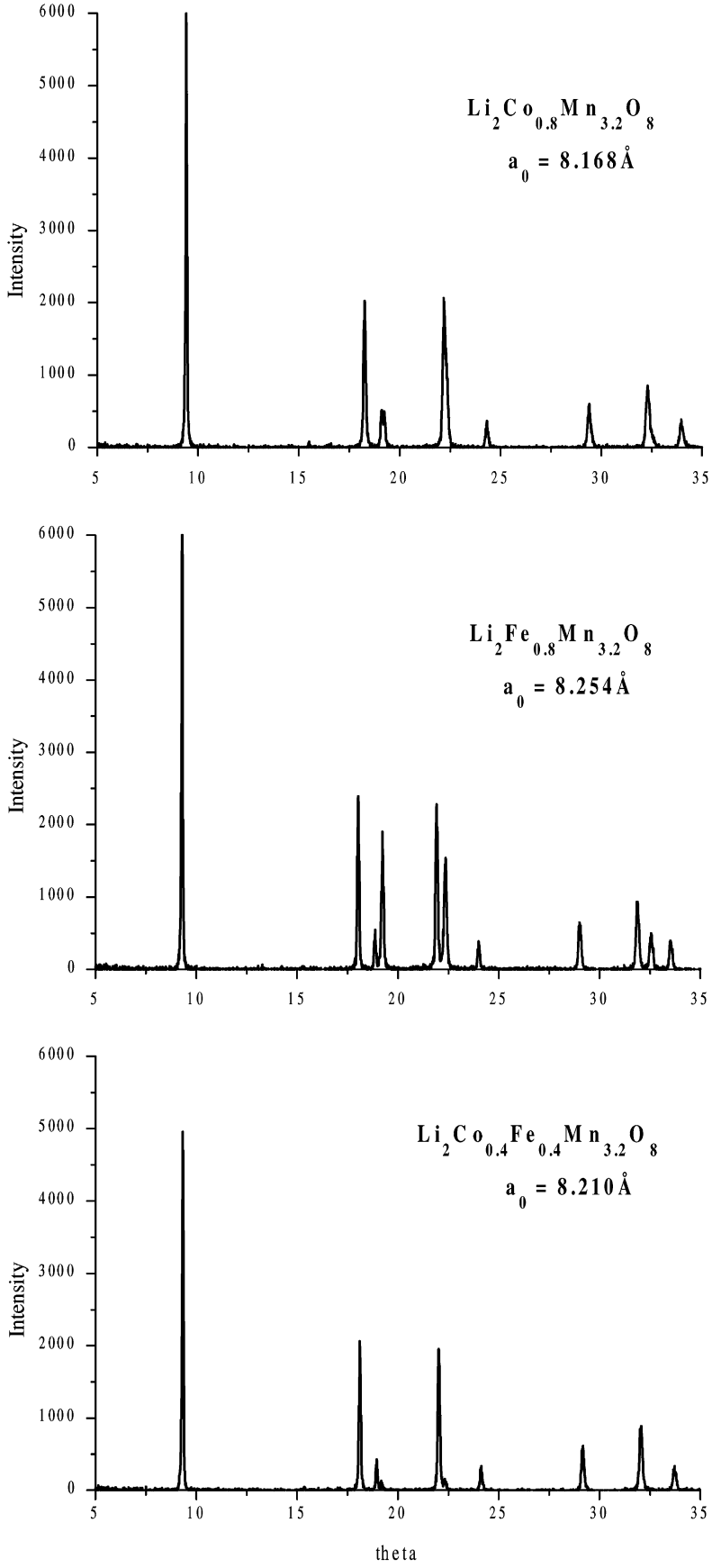

Fig. 2. X-ray powder diffraction patterns of the $Li_2M_xMn_{(4-x)}O_8$ compounds, where M = Co, Fe, Co–Fe.

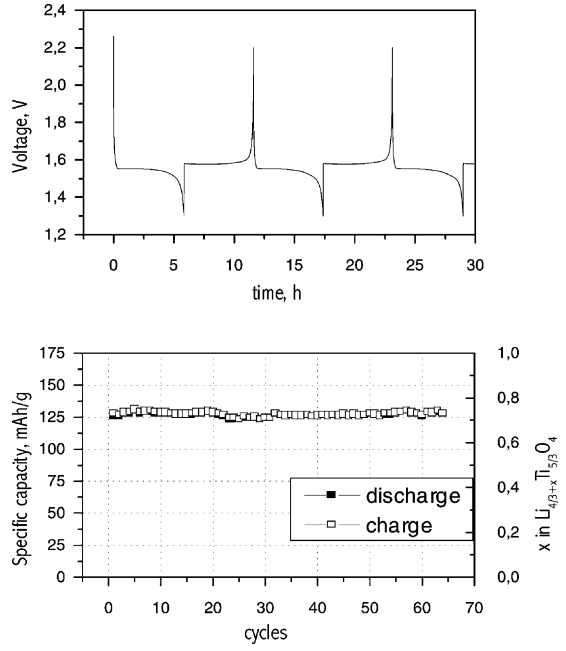

Fig. 3. Typical voltage profile of a charge–discharge cycle and related cycling capacity delivery of a $Li[Li_{1/3}Ti_{5/3}]O_4$ electrode in a $LiClO_4$ in EC–DMC electrolyte. Counter electrode: Li; room temperature; *C*/8 rate.

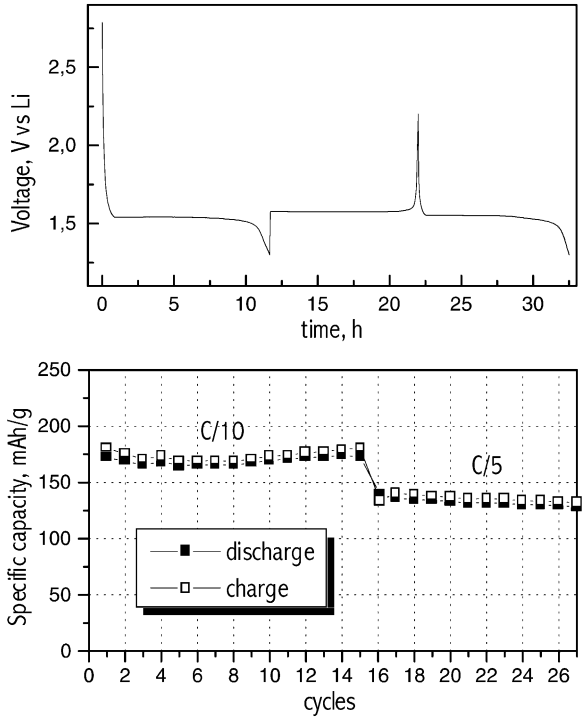

Fig. 4. Typical voltage profile of a charge–discharge cycle and related cycling capacity delivery at various rates of a $Li[Li_{1/3}Ti_{5/3}]O_4$ electrode in a $LiPF_6$ in PC electrolyte. Counter electrode: Li; room temperature.

The absence of major structural deformation makes $Li[Li_{1/3}Ti_{5/3}]O_4$ an almost ''zero strain'' electrode material characterized by a very good cyclability and by very little capacity fade upon cycling. This is confirmed by the cycling responses reported in Figs. 3 and 4. The results of these figures demonstrate that the lithium intercalation–de-intercalation process

$$Li_{4/3}Ti_{5/3}O_4 + xLi^+ + e^- \Leftrightarrow Li_{(4/3+x)}Ti_{5/3}O_4 \quad (1)$$

which involves one lithium equivalent for formula unit, evolves around 1.5 V versus Li with high reversibility, fast kinetics and with a very stable capacity delivery at various *C*-rates.

It should be noticed that one of the cycling tests (Fig. 4) was run in a cell using a $LiPF_6$ electrolyte in order to evaluate the compatibility of the $Li[Li_{1/3}Ti_{5/3}]O_4$ in the same electrolyte medium which is suitable for the operation of the $Li_2Co_{0.4}Fe_{0.4}Mn_{3.2}O_8$ high voltage cathode.

The fast kinetics of the Li-intercalation process in the defect spinel-framework $Li[Li_{1/3}Ti_{5/3}]O_4$ compound was finally determined by its impedance response. Fig. 5 shows the impedance plots of the $Li_{(4/3+x)}Ti_{5/3}O_4$ electrode at various stages of Li content, i.e. pristine ($x = 0$), in the half intercalation stage ($x = 0.5$) and back to almost total removal ($x = 0.12$), (Equation 1). It may be clearly seen that the impedance response of the electrode passes from almost purely capacitive in its pristine state, to the expected semicircle trend at the following intercalated stages. It is important to note, however, how the amplitude of the middle frequency semicircle, which is representative of the charge transfer resistance, is small (this confirming the fast kinetics of the intercalation process) and reproducible (this confirming the reversibility of the process). Furthermore, from the low-frequency Warburg linear response, one may attempt to evaluate the lithium diffusion coefficient in and out the electrode bulk. A value of about 0.8×10^{-8} cm^2 s^{-1} can be estimated from the data of Fig. 5, which is again representative of a fast mass diffusion and thus, of the very favorable electrochemical behavior of the $Li[Li_{1/3}Ti_{5/3}]O_4$ electrode.

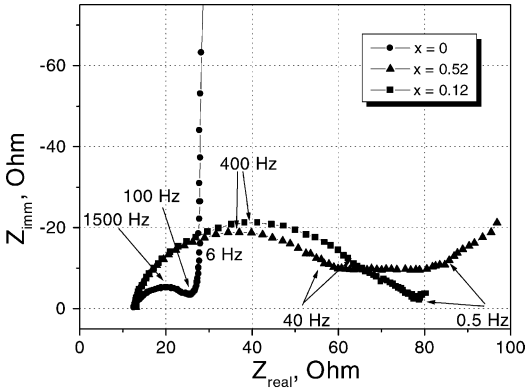

Fig. 5. Impedance plots of the $Li_{(4/3+x)}Ti_{5/3}O_4$ electrode at various stages of Li content, i.e. pristine ($x = 0$), in the half intercalation stage ($x = 0.5$) and back to almost total removal ($x = 0.12$). $LiClO_4$ in EC–DMC electrolyte. Counter and reference electrode: Li; room temperature; frequency range: 100 mHz–40 kHz.

In terms of application in a lithium-ion battery, the use of this electrode in replacement of the graphite anode versus a standard, e.g. $LiCoO_2$, cathode, would give an overall cell voltage which stabilizes around 2.5 V, i.e. about 1.5 V lower than that of the currently used lithium-ion systems. The difference is in the voltage levels of the two anode materials, i.e. 1.5 V versus Li for $Li[Li_{1/3}Ti_{5/3}]O_4$ and 0.050 V versus Li of graphite. However, the trend in the electronics circuitry of the devices where lithium-ion batteries are generally directed, foresees that the voltage powering request is going to be progressively reduced from the initial 4 V to 3 V and, possible, even to a lower range. This may somewhat eliminate the need of high voltage power sources, and thus the constraint of choosing low voltage anodes, and in turn opens new chances for selected materials operating within the stability window of the electrolyte, such as the $Li[Li_{1/3}Ti_{5/3}]O_4$ above discussed, with important advantages in terms of cyclability and safety.

In addition, the effective use of graphite with polymer electrolytes is contrasted by its hydrophobic nature. On the contrary, the $Li[Li_{1/3}Ti_{5/3}]O_4$ electrode appears in principle much more compatible with solid-like, polymer electrolytes. This is confirmed by Fig. 6 which shows the cycling response of the electrode in a cell using a $LiClO_4$–EC–PC–PAN membrane electrolyte. The same features of fast kinetics and long cyclability at various *C*-rates observed with the liquid electrolyte cells are reproduced in the polymer cell as well.

In summary, the features of the $Li[Li_{1/3}Ti_{5/3}]O_4$-type electrodes are essentially: (i) no appreciable changes in the solid host matrix upon Li uptake and release, which result in fast kinetics and high cyclability; (ii) operation above the electrolyte decomposition voltage, which results in the absence of any irreversible side reactions and (iii) high compatibility with the polymer electrolyte, which results in versatility of cell configurations. Some issues remain, which are: (i) the relatively low specific capacity which ranges around 120 mAh g^{-1} and (ii) the high operational potential, which averages around 1.5 V versus Li, both reflecting in an overall decay in energy density content. The capacity issue is of greater concern than the voltage one, due to the considerations above discussed. However, the expected high safety associated with the absence of irreversible capacity and the effective use in polymer cells, make this class of defect spinel-framework Li-insertion compounds of particular interest for the progress of lithium-ion battery

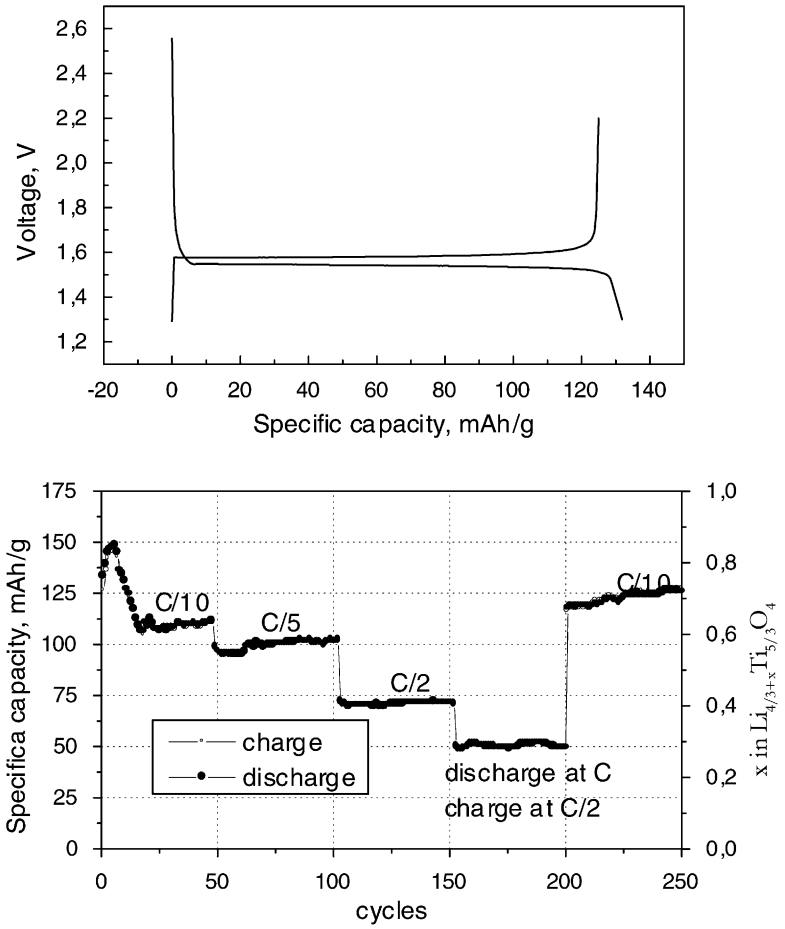

Fig. 6. Typical voltage profile of a charge–discharge cycle and related cycling capacity delivery at various rates of a $Li[Li_{1/3}Ti_{5/3}]O_4$ electrode in a $LiClO_4$–EC–DMC–PAN polymer electrolyte. Counter electrode: Li; room temperature.

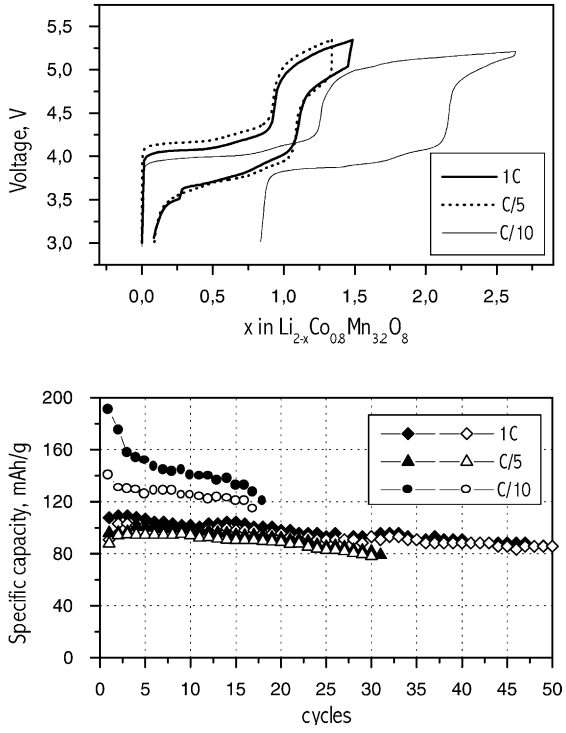

Fig. 7. Typical voltage profiles of charge–discharge cycles and related cycling capacity delivery at various rates of a $Li_2Co_{0.8}Mn_{3.2}O_8$ electrode in a $LiPF_6$ in PC electrolyte. Counter electrode: Li; room temperature.

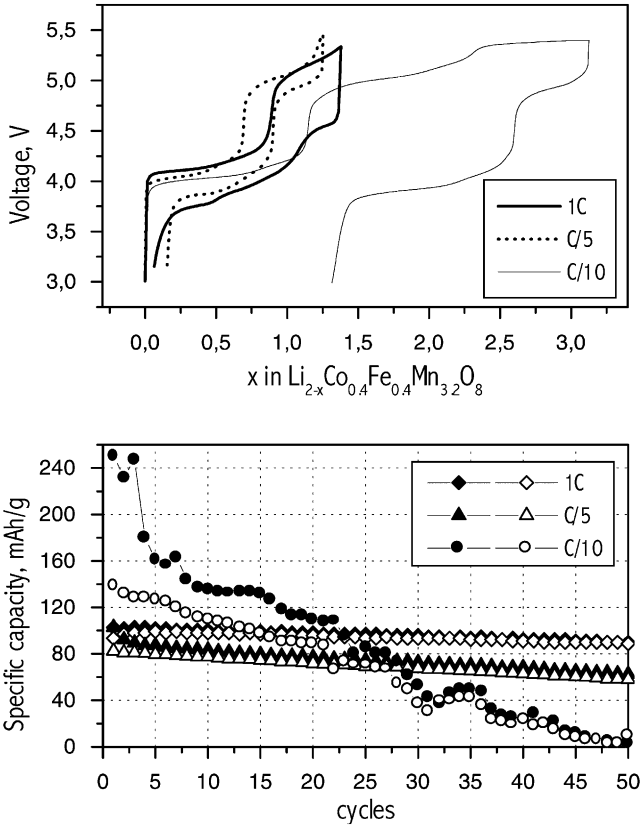

Fig. 8. Typical voltage profiles of charge–discharge cycles and related cycling capacity delivery at various rates of a $Li_2Co_{0.8}Fe_{0.4}Mn_{3.2}O_8$ electrode in a $LiPF_6$ in PC electrolyte. Counter electrode: Li; room temperature.

technology, also considering the possible compositional modifications which may allow the development of alternative compounds with higher specific capacity without jeopardizing the safe operation.

Another class of novel lithium-ion electrode materials to which great attention is presently devoted is that of the so-called" high voltage" cathodes, i.e. of electrodes which may operate in the 5 V versus Li range. In this area we have considered in some details the $Li_2M_xMn_{(4-x)}O_8$ family, where M = Fe, Co, Co–Fe [21].

Figs. 7 and 8 show the cycling response of two members of the family, i.e. the $Li_2Co_{0.8}Mn_{3.2}O_8$ and $Li_2Co_{0.4}Fe_{0.4}Mn_{3.2}O_8$ compounds, in a lithium cell using the $LiPF_6$–PC solution as electrolyte. The voltage-capacity trends demonstrate the two stages of the Li intercalation–de-intercalation

$$Li_2M_xMn_{(4-x)}O_8 \Leftrightarrow Li_{2-y}M_xMn_{(4-x)}O_8 + yLi^+ + ye^- \quad (2)$$

electrochemical process, which evolves along a first plateau (probably associated with the Mn redox process) around 4 V, followed by a second plateau evolving around 5 V versus Li. As originally reported by West and co-workers [21], the extent of the high voltage, second plateau depends on the type of the M metals. The two plateaux are reversible, suggesting fast kinetics for both processes; this is further confirmed by the scarce difference in the voltage profiles when passing from the *C*/5 to *C*/10 rate. In addition, a good capacity associated with the high potential region, is also shown.

The kinetics of the $Li_2M_xMn_{(4-x)}O_8$ electrodes have been further studied by impedance spectroscopy for the specific case of the mixed $Li_2Co_{0.4}Fe_{0.4}Mn_{3.2}O_8$ member of the family. Fig. 9 shows the impedance plots of this electrode at various stages of Li content, i.e. pristine ($x = 0$), at various de-intercalation stages and back to half of total insertion ($x = 0.5$), (Equation 2). Again, the impedance response of the electrode passes from almost purely capacitive in its pristine state, to the expected semicircle-shaped trend at the various intercalated stages. In the case of the $Li_2Co_{0.4}Fe_{0.4}Mn_{3.2}O_8$ electrode examined, here the amplitude of the middle frequency semicircle, which is representative of the charge transfer resistance, is wider than that observed for the $Li_{(4/3+x)}Ti_{5/3}O_4$ electrode discussed above this suggesting slower kinetics of the intercalation process. However, the impedance responses are similarly reproducible, this confirming that the reversibility of the process of the $Li_2Co_{0.4}Fe_{0.4}Mn_{3.2}O_8$ electrode is also quite high. As discussed, above the fitting of the low-frequency Warburg linear response may lead to the evaluation of the value of the diffusion coefficient of the order of about 5×10^{-10} cm^2s^{-1} at room temperature.

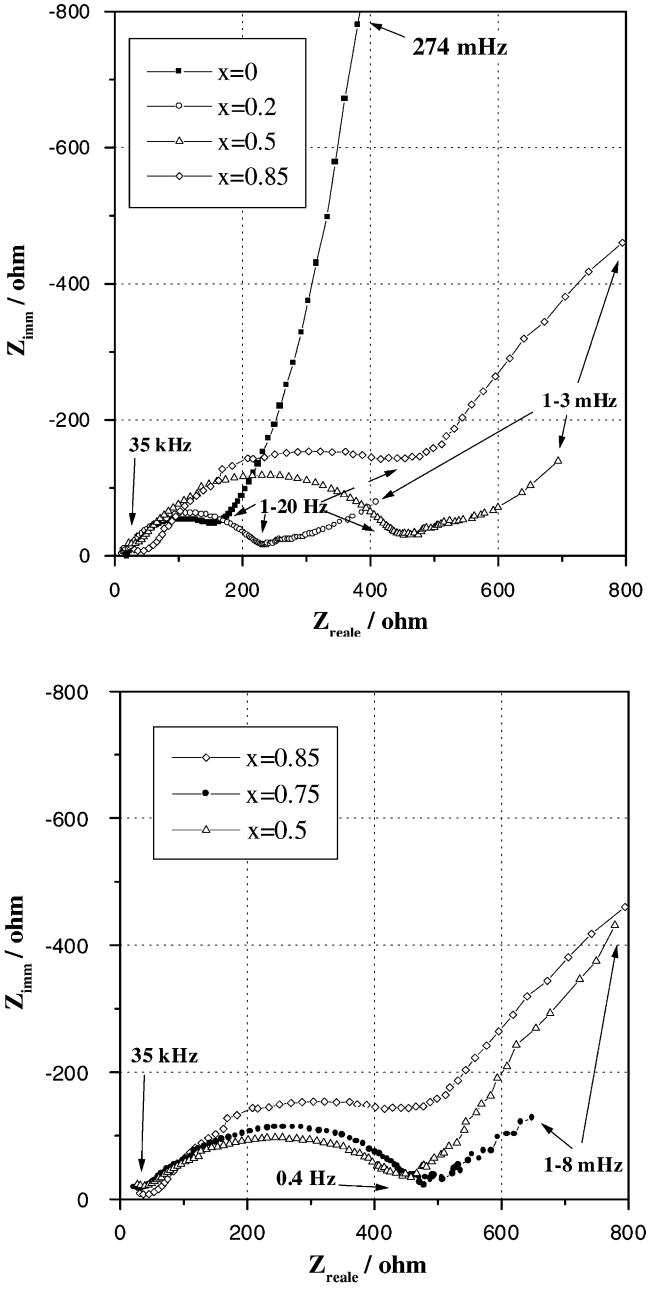

Fig. 9. Impedance plots of the $Li_2Co_{0.8}Fe_{0.4}Mn_{3.2}O_8$ electrode at various stages of Li content, i.e. pristine ($x = 0$), at various de-intercalation stages and back to half of total insertion ($x = 0.5$). $LiPF_6$ in PC electrolyte. Counter and reference electrode: Li; room temperature; frequency range: 100 mHz–40 kHz.

Figs. 7 and 8 also report the capacity delivery by the $Li_2M_xMn_{(4-x)}O_8$ electrodes upon cycling. Although reasonably stable, the $LiPF_6$–PC electrolyte still suffers of decomposition when held at voltages higher than 5 V. Thus, a definite decay in capacity is observed when the electrodes are cycled at low rates, i.e. at regimes which involve longer holding times at the high voltage range. Clearly, the proper use of these electrode materials requires the availability of an electrolyte solution having a stability window large

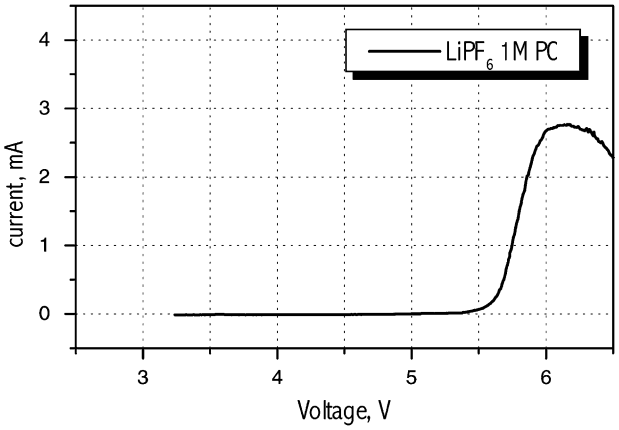

Fig. 10. Sweep voltammetery of a Super P electrode in a $LiPF_6$–PC electrolyte. Counter and reference electrode: Li; room temperature; scan rate: 0.1 mV s^{-1}.

enough to allow 5 V electrode operation. The choice of electrolytes having a high oxidation stability is restricted to few cases and even these are not always completely satisfactory. In our investigation, we have considered an electrolyte solution formed by dissolving $LiPF_6$ in propylene carbonate, PC, i.e. by selecting the salt and the solvent which are expected to be the most stable candidates among the known lithium liquid electrolyte materials. This is somewhat confirmed by Fig. 10 which shows the sweep voltammetry on $LiPF_6$–PC solution at a (Super P) carbon working electrode. The onset of the current, which is representative of the electrolyte decomposition, occurs over 5 V versus Li. However, it is important to note that the decomposition voltage at an inert electrode material such as (Super P) carbon, may be different than that occurring at the more active oxide surface of the composite $Li_2M_xMn_{(4-x)}O_8$ electrode films. Indeed, a close examination of the cycles of Figs. 7 and 8 reveals that the cell voltage flattens at the final part of the charge process, which we attribute to a partial oxidation of either the solvent, the electrolyte or both.

The results reported here show that lithium can be extracted from the $Li_2M_xMn_{(4-x)}O_8$ spinel structures along two main potential regions which vary around 3.9–4.4 V and 4.5–5.2 V versus Li, the upper voltage depending on the nature of the metal ion M, the Fe-based spinels assuring the highest capacity. At the same time, the reversibility upon cycling in the 5 V region increases with the use of the double metal oxide $Li_2Co_{0.4}Fe_{0.4}Mn_{3.2}O_8$. Indeed, the Co–Fe doping seems to have a synergetic effect to the improvement of the cycling life, which may represent the first step to the real application of the 5 V cathode materials in future-design, high energy Li-ion batteries. Presently, the full exploitation of these 5 V cathodes is somewhat hindered by the lack of suitable electrolyte media. Indeed, the role of these electrodes in the lithium-ion technology will become clearer when highly stable electrolytes will be characterized. Under these circumstances, high voltage cathodes, e.g. $Li_2Fe_{0.4}Co_{0.4}Mn_{3.2}O_8$, may be coupled with high voltage anodes,

e.g. $Li_4Ti_5O_{12}$, to form innovative lithium-ion combinations averaging around 3.5 V. A preliminary demonstration of this concept has been recently proposed by our laboratory [22].

Acknowledgements

The authors would like to thank Yuasa Corporation, Osaka, Japan for the partial financial support of this work.

References

[1] S. Megahed, B. Scrosati, J. Power Sources 51 (1994) 79.
[2] S. Megahed, B. Scrosati, Interface 4 (1995) 34.
[3] Vincent, C.A., Scrosati, B., Modern Batteries: an Introduction to Electrochemical Power Sources, 2nd Edition, Arnold, London, 1997.
[4] M. Wakihara, O. Yamamoto (Eds), Lithium-Ion Batteries, Kodansha & Wiley-VCH, Wenheim, 1998.
[5] S. Panero, G. Savo, B. Scrosati, Electrochem. Solid State Lett. 2 (1999) 365.
[6] C. Chi, C.R. Martin, B. Scrosati, J. Power Sources 97–98 (2001) 240.
[7] S.D.' Andrea, S. Panero, P. Reale, B. Scrosati, Ionics 6 (2000) 127.
[8] S. Panero, P. Reale, B. Scrosati, V. Rossi Albertini, Phys. Chem. Chem. Phys. 3 (2001) 845.
[9] F. Croce, F. Nobili, A. Deptula, W. Lada, R. Tossici, A. D'Epifanio, B. Scrosati, R. Marassi, Electrochem. Commun. 1 (1999) 605.
[10] B. Scrosati, Electrochim. Acta 15/16 (2000) 2461.
[11] S. Panero, P. Reale, F. Bonino, M. Arrabito, S. Bodoardo, D. Mazza, N. Penazzi, Solid State Ionics 128 (2000) 43.
[12] F. Bonino, S. Panero, D. Satolli, B. Scrosati, J. Power Sources 97–98 (2001) 389.
[13] F. Croce, G.B. Appetecchi, L. Persi, B. Scrosati, Nature 394 (1998) 456.
[14] F. Croce, R. Curini, A. Martinelli, L. Persi, F. Ronci, B. Scrosati, R. Caminiti, J. Phys. Chem. B 103 (1999) 10632.
[15] G.B. Appetecchi, F. Croce, G. Dautzenberg, F. Gerace, S. Panero, F. Ronci, E. Spila, B. Scrosati, Gazz. Chim. It. 126 (1996) 405.
[16] G.B. Appetecchi, F. Croce, P. Romagnoli, B. Scrosati, U. Heider, R. Oesten, Electrochem. Commun. 1 (1999) 83.
[17] G.B. Appetecchi, P. Romagnoli, B. Scrosati, Electrochem. Comm. 3 (2001) 281.
[18] T. Ohzuku, A. Ueda, N. Yamamoto, J. Electrochem. Soc. 142 (1995) 1431.
[19] T. Ohzuku, T. Yanagawa, M. Kouguchi, J. Electrochem. Soc. 142 (1995) 4033.
[20] F. Ronci, B. Scrosati, V. Rossi-Albertini, P. Perfetti, Electrochem. Solid State Lett. 3 (4) (2000) 174.
[21] H. Kawai, M. Nagata, H. Kageyama, H. Tukamoto, A.R. West, Electrochim. Acta. 45 (1999) 315.
[22] S. Panero, D. Satolli, M. Salomon, B. Scrosati, Electrochem. Commun. 2 (2000) 810.